Impact of Geometry and Satellite Mobility on Handover Strategies for Remote Driving

Giuseppe Avino*, Mario Franke†, Enric Pardo*, Christoph Sommer†, and Ion Turcanu*

*Luxembourg Institute of Science and Technology (LIST), Luxembourg

†TU Dresden, Faculty of Computer Science, Germany

{ giuseppe.avino, enric.pardo-grino, ion.turcanu }@list.lu

https://www.cms-labs.org/people/ { franke , sommer }

Abstract—Remote driving relies on continuous Vehicle-to-Satellite (V2S) connectivity in areas lacking terrestrial coverage. While early research focuses on latency and reliability for teleoperation – often evaluated under static or simplified setups – these metrics depend on specific channel models and access schemes. This paper instead provides a technology-agnostic analysis of connectivity dynamics that govern Handovers (HOs) in Low Earth Orbit (LEO) satellite networks. Using a high-fidelity simulator with satellite mobility, vehicle movement, and urban obstructions, we evaluate Line-of-Sight (LoS) availability and HO frequency under different strategies. Results show that obstruction topology and HO triggers significantly affect link continuity, with obstacle height having a non-linear impact on HO rates. A key takeaway is also that advance knowledge of satellite and vehicle trajectories can enable more intelligent HO strategies, but only if local obstruction geometry is also considered. These insights establish a baseline for future studies that integrate detailed channel models and assess end-to-end performance.

Index Terms—LEO Satellites, Teleoperated Driving, Vehicle-to-Satellite Communication, Handover Management

I. INTRODUCTION

In recent years, Connected and Automated Vehicles (CAVs) have attracted the interest of the scientific community as an exciting yet challenging area of research. Indeed, autonomous vehicles are expected to be the future of transportation, promising to enhance mobility, improve road efficiency, reduce emissions, and decrease traffic fatalities. However, practical limitations and regulatory setbacks have slowed their adoption and large-scale deployment.

In light of this, teleoperated or remote driving has emerged as a viable intermediate solution that can bridge the gap between human-driven vehicles and fully autonomous systems [1, 2]. By enabling remote control, teleoperated driving can increase safety and driving efficiency, especially in critical scenarios. To succeed, teleoperated driving depends on robust network connectivity between vehicles and remote control centers. Connectivity requirements highlighted in 3GPP studies include low latency, high reliability, and continuous coverage [1].

While 5G networks can meet these latency and reliability requirements – 3GPP began standardizing cellular support for vehicular communications with Cellular Vehicle-to-Everything (C-V2X) in Release 14 [3] – they are still too sparsely deployed. In many areas, such as rural, remote, or post-disaster regions, terrestrial coverage is limited or absent. This connectivity gap has led to growing interest in leveraging Low Earth Orbit (LEO) satellite constellations, which can provide global coverage, including in remote and infrastructure-less areas that are difficult to serve with terrestrial networks.

At the same time, several challenges arise when relying on direct Vehicle-to-Satellite (V2S) communications. Both vehicles and satellites are moving while the environment introduces obstructions such as buildings in urban scenarios that can interrupt Line-of-Sight (LoS). As a result, maintaining stable connectivity in such dynamic scenarios becomes difficult. Vehicles must be associated with the satellite that currently provides the best link conditions, which in turn may require frequent Handovers (HOs) as network dynamics and visibility conditions change [4].

Early research of teleoperated driving emphasizes latency and reliability performance with respect to 3GPP requirements. However, such metrics strongly depend on the underlying channel model and access technology, making it difficult to derive results that generalize across different systems. In this paper, we adopt a complementary perspective: we abstract away from detailed channel modeling and instead focus on the fundamental factors that govern satellite connectivity in mobility-constrained environments. Specifically, we analyze the availability of LoS links and the frequency of satellite HOs under realistic vehicle and satellite mobility conditions.

This leads to several key questions:

- What are the main factors that drive HOs in V2S communications?
- How useful is knowledge of satellite trajectory, vehicle mobility, and obstruction geometry for HO decisions?
- How should a vehicle balance frequent HOs to maintain connectivity against the overhead of excessive switching?
- How many satellites are typically visible to a moving vehicle at any given time?

To answer these questions, we conduct a baseline evaluation using a high-fidelity simulator that includes realistic models of satellite motion, vehicle mobility, and urban obstacles, while considering a range of HO mechanisms. Our results highlight how HO strategies impact satellite link availability and HO frequency. These findings provide a technology-agnostic baseline for designing more intelligent HO strategies and can serve as a foundation for future studies that integrate specific channel models and evaluate end-to-end metrics such as latency and reliability.

II. Related Work

Teleoperated driving enables remote human intervention for autonomous vehicles in edge-case scenarios, such as sensor failure, ambiguous traffic situations, or unmapped environments (e.g., post-disaster areas), ensuring safety and operational continuity when on-board Artificial Intelligence (AI) reaches its limits [2, 5]. Georg et al. [6] develop methods to measure and minimize end-to-end latency in vehicle teleoperation systems by analyzing actuator and sensor delays. More broadly, teleoperation is not limited to terrestrial vehicle networks or single vehicle control: Aggravi et al. [7] design a decentralized connectivity maintenance algorithm for multi-Unmanned Aerial Vehicles (UAVs) teleoperation to enhance safety and usability.

To ensure smooth teleoperation, ultra-low-latency communication is essential. To this end, Kuru [8] develops a human-in-the-loop teleoperation system for autonomous vehicles that combines digital twins and tactile Internet technologies to enable real-time remote intervention in edge-case scenarios. 5G networks have emerged as a solution to meet the connectivity requirements for simultaneous teleoperation communication. Limani et al. [9] demonstrate that 5G enables reliable vehicle teleoperation with cross-border capabilities, enhanced by smart infrastructure for near-physical driver awareness, while Turcanu et al. [10] show that its energy inefficiencies require 6G digital twins for sustainable ultra-reliable operation.

Given the limitations in coverage and bandwidth of terrestrial networks, in recent years, LEO satellite communication has gained interest. Li et al. [11] propose an energy-efficient LEO-based vehicular edge computing system that offloads intensive tasks to satellites, providing global coverage, low latency, and reduced power consumption for connected vehicles, with field trials validating rural emergency communications. A downside of LEO satellite-based communication is that it requires frequent HOs. Chen et al. [12] propose a Nash HO strategy, using multi-agent reinforcement learning.

Simulation studies have also gained attention. Ma et al. [13] develop a simulation framework combining satellite and vehicle mobility to evaluate LEO satellite communications for connected vehicles. Their results show that the simulated system can achieve performance comparable to that reported for Starlink, even though obstacle effects are not considered. Franke and Sommer [14] show that building geometry and urban layouts create systematic patterns in V2S connectivity, with building height and street orientation significantly affecting signal availability – while also confirming that LEO constellation density, ground station placement, and satellite inclination critically influence performance in cities. Such works open up the possibility of exploring questions around how best to take HO decisions in a V2S communication scenario.

In contrast to existing work, our study investigates HO dynamics in realistic urban environments where vehicle mobility, satellite orbital motion, and obstacle-induced LoS disruptions jointly shape connectivity. By deliberately abstracting away complex physical-layer effects, we focus on isolating the impact of HO strategies, mobility, and visibility patterns. We offer
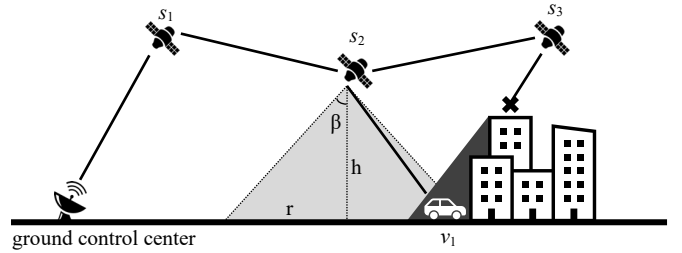

Figure 1. Use case overview. Vehicles v_i receive beacons from satellites s_j and use these beacons to determine the best satellite to offload data for a Ground Control Center (GCC). Radio reception is limited by the antenna opening half-angle β of satellites and by buildings that block radio transmissions.

a comparative analysis of benchmark HO mechanisms in scenarios characterized by highly dynamic LoS conditions and frequent satellite transitions, thus providing practical insights into the design of robust V2S communication systems for teleoperated driving.

III. Use Case Description

The use case considered in this work includes three types of nodes: vehicles, LEO satellites, and a Ground Control Center (GCC), where vehicle status data must be periodically and frequently transmitted for monitoring, command, and control purposes. Vehicles move in a remote area with no terrestrial coverage (e.g., public protection and disaster relief scenario). Therefore, the communication between vehicles and the GCC is enabled by LEO satellites, as shown in Figure 1.

Two types of messages are considered in this use case: Satellite Beacon Messages (SBMs) and Vehicle Status Messages (VSMs). SBMs contain identification information (e.g., IP, satellite ID) and are periodically sent in broadcast by LEO satellites to announce their presence to ground nodes. Each ground node, i.e., vehicle or GCC, maintains a local table of *visible* satellites, i.e., satellites from which SBMs are received.

VSMs are periodic status messages sent by each vehicle in unicast via a gateway satellite to the GCC. For example, a VSM can encapsulate a Cooperative Awareness Message (CAM), which is a well-known standardized message type in vehicular networks, that carries information such as position, speed, and heading [15]. This allows the GCC to monitor the vehicles in real time in order to provide efficient and up-to-date teleoperation commands. In this paper, we consider only the data offloaded from the vehicles to the GCC and analyze the performance of the V2S links. This approach allows us to thoroughly evaluate the most critical link of the communication chain, as it is subject to vehicle mobility and environmental obstacles, unlike the GCC-to-satellite link, where the GCC is assumed to be fixed and has dedicated satellite infrastructure.

IV. Handover Mechanisms

To ensure the communication continuity and reliability, it is essential to implement effective HO strategies that can facilitate the identification of the most suitable satellite to which each ground node should connect, and when to switch to another

Handover Mechanism	Trigger	Satellite Selection
FHO: Fixed Interval Handover	Periodic every t_w	Highest instantaneous elevation angle
IHO: Interrupted Stream Handover	n consecutive lost beacons	Highest instantaneous elevation angle
MHO: Mobility-Aware Handover	n consecutive lost beacons	Longest predicted visibility duration considering mobility
Best-Case Baseline	n consecutive lost beacons	MHO, but also considering building geometry

available node if necessary. The main factors affecting satellite selection include vehicle and satellite mobility and the presence of obstacles. Vehicles consider a satellite s_i to be *available* if its last received beacon is fresher than a threshold t_s: if so, it is selected as a candidate HO target.

In this paper, we evaluate three prototypical HO mechanisms and a best-case baseline, summarized in Table I and detailed in the following. Note that the HO process is currently modeled as instantaneous and error-free, neglecting any service interruption or delay; modeling such effects is left for future work.

A. Fixed Interval Handover (FHO)

The Fixed Interval Handover (FHO) mechanism follows a fixed periodic schedule: HOs can only be performed once every t_w, where t_w defines a fixed time window duration (e.g., 1 s, 10 s). At each HO re-evaluation, if a satellite with a higher elevation angle is available, an HO is triggered and the ground node switches to that satellite; otherwise, the ground node remains connected to the currently serving satellite. If no satellites are available when the HO re-evaluation is performed, then the ground node will remain out of coverage for the entire t_w. Similarly, if the connection to the serving satellite is lost within the fixed time window t_w, the ground node will remain disconnected for the remainder of the window.

B. Interrupted Stream Handover (IHO)

The Interrupted Stream Handover (IHO) mechanism requires that vehicles maintain a connection to the currently serving satellite s_i until n consecutive beacons from this satellite are lost. When this happens, the ground node checks the currently visible satellites and connects to the one providing the highest instantaneous elevation angle, if available. If no satellites are currently available, the ground node checks for new beacons every 100 ms (i.e., the periodicity with which satellites broadcast beacon messages), until it either connects to a new satellite s_j or reconnects to the previous satellite s_i. During the time that no beacons are received, the ground node remains out of coverage.

C. Mobility-Aware Handover (MHO)

The Mobility-Aware Handover (MHO) mechanism follows the same triggering logic of the IHO, meaning that HO re-evaluations are not performed until n consecutive beacons are lost from the serving satellite. When this occurs, however,

unlike IHO, each vehicle leverages perfect knowledge of its own planned path and the satellites' trajectories to estimate which satellite – among the currently available ones – will provide the longest connectivity window, assuming the absence of buildings that could obstruct LoS connectivity. This mechanism aims to maximize the total connection duration between ground nodes and satellites, thereby minimizing the number of needed HOs. As in the IHO mechanism, if no satellites are heard during the HO, the ground node continues to listen for new beacons every 100 ms, in order to re-establish the connection with a satellite.

D. Best-Case Baseline

To compare the performance of the three prototypical strategies and assess how far they deviate from optimal performance, we define a best-case baseline, representing the upper bound of achievable performance. While MHO relies on complete knowledge of vehicle and satellite trajectories, it neglects any information about buildings in the scenario. The best-case baseline accounts exactly for this by perfectly predicting not just vehicle and satellite mobility but also the impact of building geometry on LoS along the route.

V. SIMULATION SETUP

A. Simulation Environment

The simulation study in this paper is based on version 0.3 of the *space_Veins* framework[1]. Built on top of the widely used *Veins* framework – which couples the OMNeT++ discrete-event network simulator with the SUMO road traffic simulator – space_Veins integrates a realistic LEO satellite mobility model [16] and adapts V2S communication components from the *INET* model suite.

Specifically, space_Veins supports LEO satellite mobility through the Simplified General Perturbations 4 (SPG4) model, which calculates satellite trajectories using publicly available NASA/NORAD Two-line Element Set (TLE) data. TLE files contain key orbital parameters such as satellite name, timestamp, and trajectory data. Based on this input, space_Veins can insert multiple satellites into the simulation and continuously update their positions using the SPG4 model. By transforming the Earth-centered inertial positions of the SGP4 model into positions relative to the origin of OMNeT++'s coordinate system, established communication models (e.g., from INET) can be used to simulate V2S communication. For a more accurate and detailed description of the integration of LEO satellites within the space_Veins framework, we refer the reader to the work of Franke and Sommer [16].

B. Channel Model

We adopt a simplified channel model where transmissions are always successful unless the LoS is blocked by buildings or the ground node lies outside the coverage of all satellites.

This abstraction deliberately omits factors such as path loss (implicitly assumed sufficient whenever LoS exists), fading,

---

[1]Full source code available at https://sat.car2x.org/
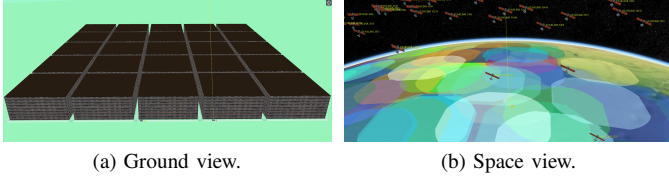
(a) Ground view.　　　　(b) Space view.

Figure 2. Simulation scenario: (a) ground view of the 5x5 Manhattan Grid; (b) space view of the Starlink constellation and its ground coverage (as rendered by LEOVISTA [19]).

Parameter	Value
Simulation length	315 s
Number of vehicles	50
Number of satellites	57
VSM size	1000 Byte
VSM interval	0.1 s
SBM size	100 Byte
SBM interval	0.1 s
Beacon loss threshold n (IHO/MHO)	3
Beacon freshness threshold t_s	0.3 s
HO mechanisms	{ IHO, FHO, MHO, baseline }
FHO re-evaluation time window t_w	{ 0.1, 1, 10, 30, 60 } s
Satellite antenna half-angle β	{ 30, 60 } °
Building height	{ 0, 20, 40, 60, 80, 100 } m
Simulation iterations	10

Doppler shift, interference, and antenna gain variations. The rationale for this simplification is to isolate the impact of HO strategies without binding the results to specific assumptions about carrier frequency, transmission power, or channel access technology. By decoupling HO dynamics from radio-layer details, the analysis remains broadly applicable across different standards and configurations. The evaluation of latency, reliability, or other end-to-end performance metrics under realistic channel models is left for future work.

C. Satellite Coverage Model

In the considered system model, we assume a service architecture based on Non-Geostationary Orbit (NGSO) satellites equipped with fixed, non-steerable beams. In such configurations, coverage footprints inherently move across the Earth's surface as a function of the satellite's orbital motion. According to the 3GPP specifications [17], this behavior corresponds to the *Earth-moving* service link type, which is characterized by coverage areas that shift relative to the Earth due to the fixed orientation of the beams with respect to the satellite platform.

A key parameter that determines the footprint radius r on Earth is the antenna opening half-angle β, which defines the beamwidth (as shown in Figure 1). A smaller aperture allows the power to be directed over a narrower area, improving signal strength. Conversely, a larger antenna aperture spreads the power over a larger area, thereby increasing coverage. The radius r is also affected by the satellite's orbital altitude h. Under the flat-Earth assumption adopted in this study – valid given the relatively small simulated area, as discussed in Section V-D – the footprint radius in simulations is given by:

$$r = h \tan(\beta) \qquad (1)$$

D. Scenario and Key Parameters

The simulation scenario adopts a 5×5 Manhattan Grid layout with orthogonal north-south and east-west streets covering 1 km × 1 km (see Figure 2a). It is placed at a fictitious location corresponding to Null Island (0°N, 0°E) to provide a neutral geographic reference. While such a synthetic layout has very different characteristics than any specific city layout and such simulations have recently been demonstrated using the same simulator we used [18], the scenario is easy to reproduce and has already been demonstrated to exhibit strong inter-scenario variance depending on its location on Earth [14].

Each road has two lanes, and each lane is 3.2 m wide. Buildings are located between the roads, at a distance of 5 m.

In each simulation run, all buildings have the same height, which is varied between simulations from 0 m to 100 m in 20 m steps. This uniform-height assumption simplifies the environment while allowing controlled evaluation of how obstacle height influences LoS blockage probability and, consequently, handover dynamics.

The simulation considers 50 vehicles, with performance metrics collected only within a Region of Interest (RoI) that excludes half a building width along scenario boundaries to avoid perimeter effects. The satellite constellation is modeled as a representative Starlink deployment using a public TLE dataset containing 6776 satellites obtained from CelesTrak[2]. Only satellites with an elevation angle of at least 25° over Null Island are simulated, in accordance with Starlink regulatory requirements [20, III-E-1, para. 42], reducing the constellation to 57 satellites (see Figure 2b).

Given the average orbital altitude of the Starlink satellites of 550 km and the two values of β considered, i.e., 30° and 60°, we can apply Equation (1) to compute the satellite footprint radius r. This yields a radius of approximately 317 km for $\beta = 30°$ and about 951 km for $\beta = 60°$.

In total, we vary four parameters in our simulations: building height, satellite antenna half-angle β, HO mechanism, and, specifically for FHO, the HO re-evaluation time window t_w. For each combination of these parameters, 10 simulation iterations are performed to increase the robustness of the results. A summary of the key simulation parameters is given in Table II.

E. Mobility-Based Satellite Selection Criterion

The procedure to identify the *best* satellite is more elaborate in the MHO strategy – unlike FHO and IHO, which rely on selecting the satellite with the highest instantaneous elevation angle – and consists of three main steps:

Step 1 – Data collection. A first set of simulations is executed, where each vehicle records, at regular intervals of 100 ms, the ID of all visible satellites. Each simulation produces a CSV file containing three columns: vehicle ID, satellite ID, and tick, where a *tick* represents the integer conversion of the

---

[2]https://celestrak.org/NORAD/elements/

simulation time (e.g., 1.3428 s becomes tick 13). For this initial phase, the simulation configuration without buildings is used.

Step 2 – Post-processing and best-satellite selection. The output files generated in the first step are processed using a Python-based script, whose core algorithm is shown in Algorithm 1. For each vehicle, we first group consecutive detections of the same vehicle-satellite pair into *visibility windows W_v*, each defined by its start and end tick (t_{start}, t_{end}). A new window is opened whenever two consecutive samples are separated by more than g ticks – equal to one tick in our case (1 tick = 0.1 s). We then build a regular time grid of ticks for each vehicle to ensure full temporal coverage (from tick 0 to 3150, corresponding to a simulation length of 315 s). We then pair every grid tick with all windows of that vehicle in W_v and select, among the available satellites, the one whose window ends farthest in the future (the row with the highest t_{end}) – i.e., the satellite offering the longest remaining visibility. If no window covers a given tick, the output entry is set to null, meaning that no satellite is considered currently available. A satellite is deemed unavailable when the last received beacon is older than n beacon intervals; as discussed previously, in this study we use $n = 3$ (corresponding to a freshness threshold of 300 ms given the 100 ms beaconing period). In summary, for each vehicle and at every tick, the algorithm determines the satellite guaranteeing the longest uninterrupted visibility period. For instance, if at tick 13, satellites sat_a, sat_b, and sat_c are available for vehicle v_i, and their continuous visibility extends up to ticks 50, 53, and 38 respectively, then sat_b is selected for v_i at tick 13. This process outputs a second CSV file containing three columns: tick, vehicle ID, and the selected satellite ID.

Step 3 – Simulation with mobility-aware handover. A second round of space_Veins simulations – constituting the actual evaluation runs – is then performed using all configurations listed in Table II, including those with buildings. Whenever a ground node v_i triggers a handover, the current simulation time is converted into a tick (t_j), and the corresponding serving satellite is determined by reading the entry associated with v_i at tick t_j in the output file generated during the second step. If the selected satellite is not available (e.g., obstructed by a building), the fallback criterion from IHO and FHO is applied, selecting the satellite with the highest current elevation angle.

This design explains why the first phase is executed using the building-free configuration: it provides complete knowledge of vehicle and satellite mobilities, while assuming no knowledge about future environmental obstructions.

VI. RESULT ANALYSIS

This section presents the main outcomes of our evaluation, focusing on two key performance metrics and complemented by one auxiliary metric:

- *Link availability ratio:* the probability that the vehicle has an operational V2S connection at each 0.1-second simulation step. This condition is met if the vehicle successfully receives the satellite beacon in that step,

which implies that also the periodic VSM transmitted during the same interval is successfully delivered.

- *Number of handovers:* the average number of HOs per vehicle throughout the simulation. To compute this, we distinguish between two cases: switching to a different satellite directly and switching to a different satellite from a state of being disconnected. Directly switching to a different satellite always counts as a HO. Switching to a satellite after being disconnected only counts as a HO if the satellite differs from the previous one.
- *Number of visible satellites:* the average number of satellites available to each vehicle during the simulation. It is used to show the impact of different satellite antenna half-angles β on the HO procedure.

A. Elevation-Angle–Based Handover Performance

The IHO and FHO mechanisms rely on a basic approach to managing handovers, that does not require complex decision logic. Indeed, in both cases, when a handover is triggered, the

---

Algorithm 1 Longest Uninterrupted Visibility Satellite Selection

Input: H: set of observations (v, s, t) that vehicle v was visible to satellite s at tick t; N: simulation duration in ticks; g: maximum allowed gap (in ticks)

Output: B: rows (t, v, s) indicating that at tick t vehicle v will have longest uninterrupted connection to satellite s

1: **for all** vehicles v in H **do**
2:    $W_v \leftarrow \varnothing$ ▷ *satellite visibility windows* $(v, s, t_{start}, t_{end})$
3:    **for all** satellites s visible to vehicle v in H **do**
4:      $H_{v,s} \leftarrow (v, s, t) \in H$ for current v and s, sorted by t
5:      $t_{\text{start}} \leftarrow t_{\text{prev}} \leftarrow$ first tick t in $H_{v,s}$
6:      **for** remaining ticks t in $H_{v,s}$ **do**
7:        **if** $t - t_{\text{prev}} > g$ **then**
8:          add $(v, s, t_{\text{start}}, t_{\text{prev}})$ to W_v ▷ *close window*
9:          $t_{\text{start}} \leftarrow t$ ▷ *new window begins*
10:        **end if**
11:        $t_{\text{prev}} \leftarrow t$
12:      **end for**
13:      add $(v, s, t_{\text{start}}, t_{\text{prev}})$ to W_v ▷ *close last window*
14:    **end for**
15:    **for all** $t \in \{0, 1, 2, \ldots, N\}$ **do**
16:      $C \leftarrow \{ w \in W_v \mid w.t_{\text{start}} \leq t \leq w.t_{\text{end}} \}$ ▷ *set of all satellites whose visibility window covers the current tick for vehicle v*
17:      **if** $C = \varnothing$ **then**
18:        add (t, v, null) to B ▷ *no satellite available*
19:      **else**
20:        $\hat{w} \leftarrow \text{argmax}_{w \in C} \, w.t_{\text{end}}$
21:        add $(t, v, \hat{w}.s)$ to B ▷ *add the satellite whose visibility window ends farthest in the future*
22:      **end if**
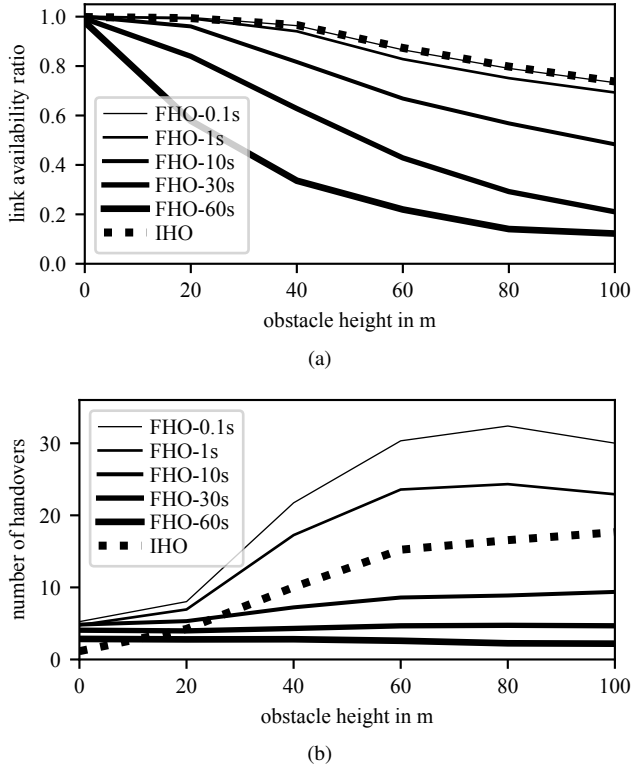23:   **end for**
24: **end for**
25: **return** B

Figure 3. Comparison of Vehicle-to-Satellite (V2S) link availability ratio (a) and number of handovers (HOs) (b) for both Interrupted Stream Handover (IHO) and Fixed Interval Handover (FHO) mechanisms, with a satellite antenna half-angle $\beta = 60°$.

vehicle selects the new satellite as the one with the highest instantaneous elevation angle among those currently available. This selection assumes that vehicles can obtain the elevation angle of all satellites from which they currently receive beacons. As shown in Figure 3a, in the absence of environmental obstacles – i.e., for an obstacle height of 0 m – the link availability ratio is close to 1 for all HO mechanisms. This is expected, since with no buildings obstructing LoS and with a relatively large satellite footprint corresponding to a half-angle aperture of $\beta = 60°$, satellites remain visible to vehicles for long periods. Consequently, even for large t_w values (e.g., 60 s), vehicles can remain attached to the same satellite without degrading link availability.

As obstacle height increases, HO strategies exhibit different behaviors. In particular, coarse FHO re-evaluation intervals lead to a rapid degradation of link availability; for example, when $t_\mathrm{w} = 60$ s, the ratio drops to 0.6 at a building height of 20 m and to nearly 0.1 at 100 m. Reducing the re-evaluation interval to 30 or 10 s mitigates this effect, although these configurations are still clearly outperformed by the lowest t_w, i.e., 1 and 0.1 s. Overall, IHO and FHO variants with short t_w achieve the highest link availability by reacting promptly to dynamic LoS changes and satellite visibility.

This observation should, however, be interpreted together with the results in Figure 3b, which depicts the average number of HOs per vehicle. Interestingly, IHO achieves high

link availability with significantly fewer handovers when compared to FHO. While both IHO and FHO-0.1s ensure a high probability of maintaining an operational satellite link – and FHO-1s follows closely – Figure 3b highlights the efficiency of IHO in minimizing unnecessary handovers. Although HO overhead is not modeled, minimizing the number of HOs can be critical, since they can fail or introduce delays or losses.

As expected, reducing the HO re-evaluation time window t_w increases the number of handovers. An interesting trend is observed for FHO-0.1s and FHO-1s: the number of HOs increases with building height up to a peak at around 80 m, after which it decreases. At low building heights, vehicles are able to maintain more stable links and thus perform fewer HOs because the impact of obstacles is limited. As building height increases, obstacles affect the LoS, requiring more frequent HOs. However, beyond the peak, the number of HOs begins to decrease due to the reduced number of visible satellites.

Overall, IHO provides the best trade-off between link availability and handover stability, while FHO-0.1s achieves similar availability at the cost of excessive handovers. Conversely, FHO-1s offers a more balanced compromise between responsiveness and stability. The remaining FHO-based configurations with larger re-evaluation windows t_w perform well only in the absence of buildings but experience significant degradation as obstacle height increases.

B. Mobility-Aware Handover & Optimal Baseline Performance

As a second step, we consider a more advanced approach for selecting the new serving satellite during an HO procedure, which accounts for the trajectories of both satellites and vehicles, as described in Section V-E. This alternative approach aims to maximize the connectivity duration and thereby reduce the number of HOs. In parallel, we define the best-case baseline scenario (Section IV-D), representing the optimal solution under full knowledge of mobility and surrounding obstacles. Having such a reference allows us to make both relative and absolute comparisons among the different mechanisms, providing a measure of how close IHO, FHO, and MHO can approach the best achievable performance.

The link availability ratio for IHO, FHO-1s[3], MHO, and the baseline is shown in Figure 4a. Both IHO and MHO closely follow the baseline, achieving near-optimal link availability across all building heights. The strong performance of IHO is attributed to its high reactivity, while MHO demonstrates that a selection strategy based on the relative mobility of satellites and vehicles can effectively preserve link availability. For FHO-1s, comparable performance is observed up to 40 m, whereas a slight degradation appears at larger building heights due to the less frequent re-evaluation interval.

As in the previous section, Figure 4a should be analyzed together with Figure 4b, which depicts the average number of HOs per vehicle – representing the *cost* of maintaining high availability. Here, differences among the strategies are

---

[3]Only FHO-1s is reported as a representative configuration, as it offers a good trade-off between link availability and the number of HOs.
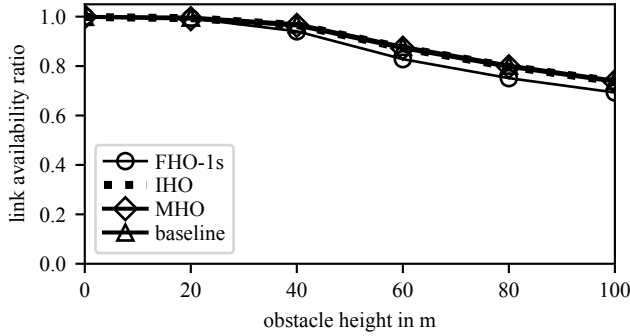
(a)
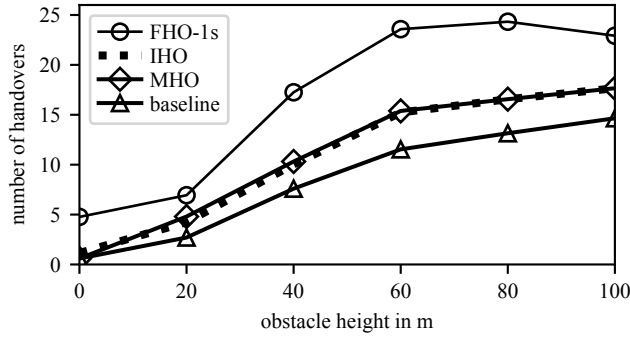
(b)

Figure 4. Comparison of Vehicle-to-Satellite (V2S) link availability ratio (a) and number of handovers (HOs) (b) for the four HO mechanisms under evaluation, with a satellite antenna half-angle $\beta = 60°$. For the FHO, we report only the case with t_w equal to 1 s.

Figure 5. Number of handovers (HOs) for the four HO mechanisms under evaluation, with a satellite antenna half-angle $\beta = 30°$. For the FHO, we report only the case with t_w equal to 1 s.

Figure 6. Average number of satellites visible to vehicles for antenna half-angles $\beta = 60°$ and $\beta = 30°$. Horizontal reference lines ($y = 1$ and $y = 2$) highlight when the average visibility equals one or two satellites, respectively.

more evident. Indeed, we can clearly observe that the baseline shows a number of HOs that none of the other strategies achieve, except in the absence of buildings. In this case indeed, the baseline and the MHO yield identical results, with IHO performing closely behind. However, even moderate obstacle heights (e.g., 20 m) cause the baseline to achieve a lower number of HOs compared to the other three strategies.

It is worth emphasizing that MHO and IHO share a very similar behavior. This similarity arises because, when the mobility-based selection (MHO) identifies a satellite that is not currently visible, the fallback criterion reverts to the highest instantaneous elevation angle – the same rule adopted by IHO.

From these results, we can conclude that IHO, MHO, and FHO-1s (and by extension FHO-0.1s) achieve excellent link availability. However, in terms of HO frequency, their performances are not as good as those of the optimal case, meaning that the latter achieves a lower number of HOs. Most notably, except in the scenario without buildings, the more complex mobility-based selection – implemented in MHO – does not yield a significant improvement over the simpler elevation-angle-based criterion leveraged by IHO. Thus, without full knowledge of the surrounding geometry, the additional computational complexity of mobility-based decisions does not provide any tangible improvement over the simpler elevation-angle criterion.
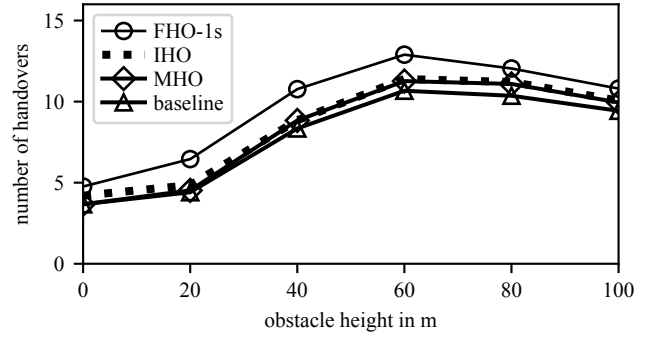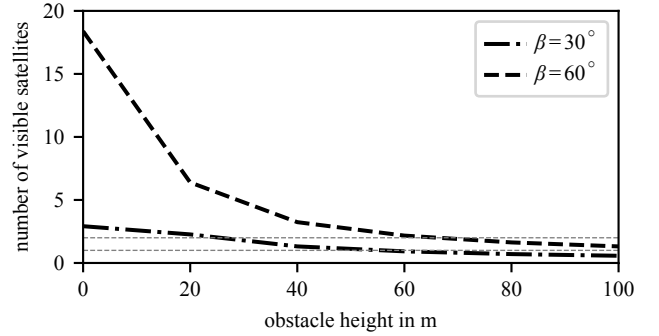
C. Impact of the Satellite Antenna Half-Angle (β)

So far, we have analyzed only the case where the satellite antenna half-angle β is equal to 60°. While the results for $\beta = 30°$ are qualitatively similar in terms of link availability ratio, showing the same overall trend, the analysis of the number of HOs, reported in Figure 5, reveals notable differences. By comparing these results with Figure 4b, we observe that the number of HOs is lower for $\beta = 30°$ across all HO mechanisms. This behavior is explained by the fact that a smaller β implies a lower beamwidth, leading to a lower number of visible satellites. Intuitively, indeed, the higher the number of visible satellites, the more opportunities vehicles have to perform HOs, as there is a wider range of satellites available to connect to.

The difference between the satellites visible for $\beta = 60°$ and $\beta = 30°$ is depicted in Figure 6, and shows a significant difference, especially in scenarios without buildings. As the building height increases, the number of visible satellites decreases, with a particularly rapid decrease for $\beta = 60°$ with 20 m-high buildings. When the obstacle height exceeds 60 m, the difference in the number of satellites visible with the two different β values becomes less pronounced.

These results help to explain why the number of HOs initially increases with building height and then begins to decrease. For example, at $\beta = 30°$ and building heights of 60 m or more, the average number of satellites visible by vehicles drops to

only one on average. Therefore, with no alternatives available, HOs cannot occur, which naturally reduces their number. For the same reason, at $\beta = 30°$, the difference in the number of HOs among the baseline, MHO, and IHO is less pronounced than that observed for $\beta = 60°$.

VII. CONCLUSION

This paper evaluated Vehicle-to-Satellite (V2S) communication for teleoperated driving over Low Earth Orbit (LEO) constellations, focusing on the impact of Handover (HO) strategies under dynamic Line-of-Sight (LoS) conditions, geometry, and satellite and vehicle mobility. We combined an abstract channel model with a high-fidelity simulator modeling realistic satellite motion, vehicle mobility, and urban obstructions to analyze handover triggers and satellite selection in HO mechanisms.

A key finding is that simple elevation-angle-based satellite selection strategies, represented by strategies *Interrupted Stream Handover (IHO)* and *Fixed Interval Handover (FHO)*, are capable of maintaining near-optimal link availability in obstacle-free scenarios. This trend holds also when building height increases, although at the cost of more frequent HOs. Conversely, longer HO re-evaluation windows for the FHO strategy result in significantly degraded link availability.

Moreover, taking into account future mobility of both vehicles and satellites – even if predicted perfectly – does not automatically yield better performance. Such an approach, represented by strategy *Mobility-Aware Handover (MHO)*, achieves performance close to the theoretical optimum only in open-sky conditions. Without information about local 3D geometry, namely surrounding buildings, the performance is no better than IHO. This indicates that without accurate building information, the additional computational complexity of MHO provides no tangible improvement over the simpler elevation-based criterion leveraged by IHO. With building information, however, the number of HOs can be substantially reduced.

We also demonstrated how antenna beamwidth and obstacle height jointly shape satellite visibility and HO frequency. The number of visible satellites plays a critical role in determining HO opportunities, explaining the non-monotonic relationship between obstacle height and HO frequency.

Overall, these findings suggest that simple, elevation-based HO strategies can deliver near-optimal performance under many conditions, whereas mobility-aware optimization becomes beneficial primarily when detailed geometry data is available.

Future work will investigate more advanced approaches, such as multi-link connectivity, along with explicit handover effects (e.g., handover time) and more detailed channel models, to enable the assessment of end-to-end performance metrics.

ACKNOWLEDGMENTS

REFERENCES

[1] 3rd Generation Partnership Project (3GPP), "Technical Specification Group Services and System Aspects; Study on enhancement of 3GPP Support for 5G V2X Services," TR 22.886, version 16.2.1, Dec. 2018.

[2] T. Zhang, "Toward Automated Vehicle Teleoperation: Vision, Opportunities, and Challenges," *IEEE Internet of Things Journal*, vol. 7, no. 12, pp. 11 347–11 354, Dec. 2020.

[3] M. H. C. Garcia, A. Molina-Galan, M. Boban, J. Gozalvez, B. Coll-Perales, T. Şahin, and A. Kousaridas, "A Tutorial on 5G NR V2X Communications," *IEEE Communications Surveys & Tutorials*, vol. 23, no. 3, pp. 1972–2026, 2021.

[4] A. M. Voicu, A. Bhattacharya, and M. Petrova, "Handover Strategies for Emerging LEO, MEO, and HEO Satellite Networks," *IEEE Access*, vol. 12, pp. 31 523–31 537, 2024.

[5] D. Majstorović, S. Hoffmann, F. Pfab, A. Schimpe, M.-M. Wolf, and F. Diermeyer, "Survey on Teleoperation Concepts for Automated Vehicles," in *2022 IEEE International Conference on Systems, Man, and Cybernetics (SMC)*, IEEE, Oct. 2022, pp. 1290–1296.

[6] J.-M. Georg, J. Feiler, S. Hoffmann, and F. Diermeyer, "Sensor and Actuator Latency during Teleoperation of Automated Vehicles," in *2020 IEEE Intelligent Vehicles Symposium (IV)*, IEEE, Oct. 2020, pp. 760–766.

[7] M. Aggravi, C. Pacchierotti, and P. R. Giordano, "Connectivity-Maintenance Teleoperation of a UAV Fleet With Wearable Haptic Feedback," *IEEE Transactions on Automation Science and Engineering*, vol. 18, no. 3, pp. 1243–1262, Jul. 2021.

[8] K. Kuru, "Conceptualisation of Human-on-the-Loop Haptic Teleoperation With Fully Autonomous Self-Driving Vehicles in the Urban Environment," *IEEE Open Journal of Intelligent Transportation Systems*, vol. 2, pp. 448–469, 2021.

[9] X. Limani, N. Slamnik-Kriještorac, T. van de Ven, and J. M. Marquez-Barja, "Optimizing 5G-based Teleoperation: Synergy of Vulnerable Road User Awareness and Advanced Traffic Management Systems," in *2024 Joint European Conference on Networks and Communications & 6G Summit (EuCNC/6G Summit)*, IEEE, Jun. 2024, pp. 1067–1072.

[10] I. Turcanu, S. Faye, H. Fellner, G. Castellanos, J. Baudouin, S. M. Senouci, M. Franke, and C. Sommer, "Digital Twinning for 6G Teleoperated Driving: The 6G-TWIN Vision," in *EuCNC & 6G Summit 2024 (EUCNC), Poster Session*, Antwerp, Belgium: Zenodo, Jun. 2024.

[11] C. Li, B. Shang, J. Feng, and S. Chen, "LEO Satellite-Assisted Vehicular Edge Computing," in *2023 3rd International Conference on Intelligent Communications and Computing (ICC)*, IEEE, Nov. 2023, pp. 157–162.

[12] J. Chen, M. Ozger, and C. Cavdar, "Nash Soft Actor-Critic LEO Satellite Handover Management Algorithm for Flying Vehicles," in *2024 IEEE International Conference on Machine Learning for Communication and Networking (ICMLCN)*, IEEE, May 2024, pp. 380–385.

[13] J. Ma, L. Zhong, and R. Onishi, "LEO Satellite Communication Simulation Framework for Connected Vehicles," in *IEEE Global Communications Conference (GLOBECOM 2023)*, IEEE, 2023, pp. 6597–6602.

[14] M. Franke and C. Sommer, "Obstacle Shadowing in Vehicle-to-Satellite Communication: Impact of Location, Street Layout, Building Height, and LEO Satellite Constellation," in *IEEE Vehicular Networking Conference (VNC)*, IEEE, May 2024, pp. 305–312.

[15] ETSI EN 302 637-2 V1.3.2 (2014-11), "Intelligent Transport Systems (ITS); Vehicular Communications; Basic Set of Applications; Part 2: Specification of Cooperative Awareness Basic Service," Nov. 2014.

[16] M. Franke and C. Sommer, "Toward Space-Air-Ground Integrated Network Simulation with 4D Topologies," in *19th Wireless On-Demand Network Systems and Services Conference (WONS)*, IEEE, Jan. 2024, pp. 61–68.

[17] 3rd Generation Partnership Project (3GPP), "NR; NR and NG-RAN Overall description; Stage-2 (Release 18)," TS 38.300, version 18.5.0, Apr. 2025.

[18] E. Zanotto and L. Maccari, "Simulating Urban Satellite-Based Vehicular Networks: Focus on Maps, Building Heights, or Vehicle Density?" In *2025 20th Wireless On-Demand Network Systems and Services Conference (WONS)*, 2025.

[19] D. Andronovici, G. Avino, M. Franke, D. Nicolas, I. Turcanu, and C. Sommer, "LEOVISTA: A Cesium-Based 3D Visualization Tool for Satellite-Enabled Vehicle Simulations," in *29th International Symposium on Distributed Simulation and Real Time Applications (DS-RT 2025)*, Prague, Czech Republic: IEEE, Sep. 2025.

[20] "Order and Authorization 22-91," Federal Communications Commission (FCC), DA/FCC 22-91, Dec. 2022, pp. 1–74.